IEEE Access
Multidisciplinary | Rapid Review | Open Access Journal

Received 7 May 2023, accepted 17 May 2023, date of publication 22 May 2023, date of current version 1 June 2023.

Digital Object Identifier 10.1109/ACCESS.2023.3278793

RESEARCH ARTICLE

Analysis of Mechanical-Hydraulic Cooperative Response of Hydraulic Support Under Roof Rotary Impact

QINGLIANG ZENG[1,2], CHEN MA[1], ZHAOSHENG MENG[3,4], PENGHUI XU[1], AND XIAOWAN LEI[1]

[1]College of Mechanical and Electronic Engineering, Shandong University of Science and Technology, Qingdao 266590, China
[2]College of Information Science and Engineering, Shandong Normal University, Jinan 250014, China
[3]State Key Laboratory of Mining Disaster Prevention and Control Cofounded by Shandong Province and the Ministry of Science and Technology, Shandong University of Science and Technology, Qingdao 266590, China
[4]College of Energy and Mining Engineering, Shandong University of Science and Technology, Qingdao 266590, China

Corresponding author: Zhaosheng Meng (skdmzs@163.com)

This work was supported in part by the National Natural Science Foundation of China under Grant 51974170, Grant 52104164, and Grant 52274132; in part by the Natural Science Foundation of Shandong Province under Grant ZR2020QE103; in part by the Key Research and Development Plan of Shandong Province under Grant 2019SDZY01; and in part by the Central Guidance for Local Science and Technology Development Fund Projects of Shandong Province under Grant YDZX2022013.

ABSTRACT Hydraulic support is a collaborative bearing equipment with hydraulic transmission power and mechanical bearing load. The method of the mechanical-hydraulic co-simulation model is used to discuss the response difference of hydraulic support in the process of roof rotation. Based on this model, the variation law of hydraulic support is analyzed by changing the rotation velocities of the roof. Then, by changing the discharge flow of relief valves at the column, the energy unloading characteristics of the column are discussed. The results demonstrate that with an increase in the roof rotary velocity, the pressure and flow peaks of the column increase continuously (the increase multiples of pressure and flow peaks are 123% and 51%, respectively). The tendency of load variation at different locations of hinge points appears to be varied. Lastly, this paper increases the discharge flow of the relief valve to shorten the energy unloading time (by 1.5 s) and reduce the load at the hinge point. This approach helps reduce the probability of damage to the hydraulic support and prolongs its life.

INDEX TERMS Hydraulic drives, mechanical engineering, valves.

I. INTRODUCTION

As an important national energy, coal mining, and utilization efficiency determine the speed of industrialization and economic development [1], [2], [3], [4]. Fig. 1 shows the working process of the hydraulic support. It can be divided into four stages, which are shown by Fig. 1A, B, C, and D, respectively. Firstly, the hydraulic support increases its height to support the roof (A); after the shearer finishes coal mining, the height of the hydraulic support decreases (B); then the shearer and the armored face conveyor move toward the coal seam with the help of the shift jack. After completing the above actions, the hydraulic support moves toward the coal seam with the pull of the shift jack (C); finally, after reaching the specified position, the hydraulic support rises again to support the roof and maintain the normal work of the working face(D). When the hydraulic support is moving, it will be continuously impacted by the dynamic effect of immediate roof crushing and caving, main roof fracture, and instability [5], [6], [7], [8]. Therefore, studying the load transfer law of hydraulic support in the impact process has a key guiding role in its selection design and performance optimization.

Numerous scholars have mainly carried out the following research works to study the influence of loading mode on the pressure and structural movement of hydraulic support systems. Szurgacz Dawid [9], [10] introduced that hydraulic

The associate editor coordinating the review of this manuscript and approving it for publication was Zheng Chen.

This work is licensed under a Creative Commons Attribution-NonCommercial-NoDerivatives 4.0 License.
For more information, see https://creativecommons.org/licenses/by-nc-nd/4.0/

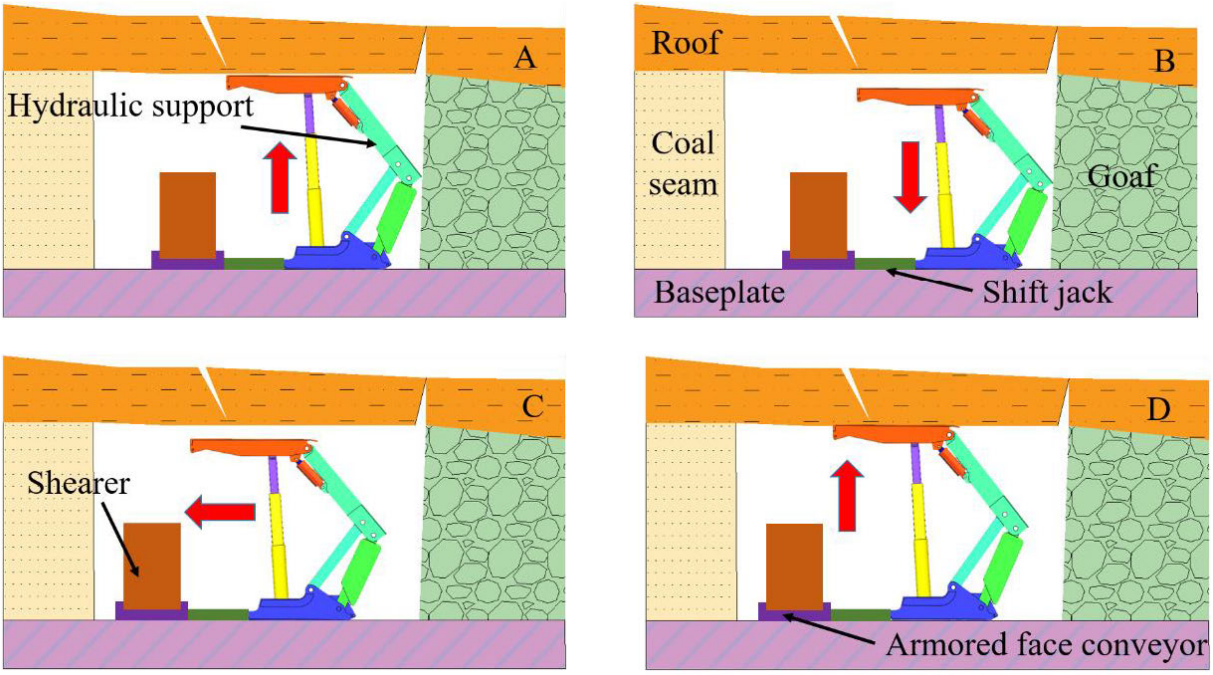

FIGURE 1. The working process of the hydraulic support.

supports are susceptible to the impact of coal seams during the bearing and caused undesirable consequences of damage to the double telescopic column. Guo and Mao [11] designed and prevented three energy-absorbing members at the top beam position to enhance the resistance of the bracket. Meng et al. [12] placed load impact points at different positions above the support to observe the overall action of the support and obtain the stress concentration position of the structural parts. Guo and Zhao [13], [14] established the mathematical model and simulation model of the safety valve. The authors compared the dynamic differences under impact conditions through simulation analysis and experimental operation. Meng and Zeng [15] established the hydraulic support impact dynamics model and discussed the influence of balancing jack position on the hydraulic support bearing capacity. Li and Andrzej [16], [17] carried out a fluid-solid coupling analysis on the established safety valve model. The results are of great significance for the parameter optimization of the hydraulic control system and the guidance of coal mine safety production. Yang et al. [18] discussed stress-sensitive regions of mechanical structures by separating or unifying the loading of the top and cover beams. Wan and Wang [19] studied the effect of gangue particles on the motion state of the bracket and obtained that the enhanced particle impact signal would change the operating characteristics of the bracket. Based on the numerical simulation and hydraulic support model impact test bench, to solve the problem of uneven distribution of energy when the support is working, Ren et al. [20] proposed a method to change the support force and stiffness of the column, which provides a basis for the performance optimization of the large cylinder column system. Based on the working principle of hydraulic support, Zhai et al. [21] established a hydraulic system model. The authors differentiated the response of the system during operation by changing the spring stiffness of the piston rod position.

In addition, the improvement in the level of computer application has promoted the progress of science and technology, making more and more industrial software serve in the development and research process of construction machinery. References [22], [23], [24], [25], [26], and [27] show that software in different fields performs co-simulation to complete product development and design. Furthermore, the co-simulation results are more accurate than single simulation results, and the obtained data results are closer to the real situation. Co-simulation technology has the advantages of improving the product design quality, shortening the new product development cycle, and reducing new product manufacturing costs. It is widely used in product performance improvement and other aspects. However, the method is less applied to the study of hydraulic supports.

To summarize, the existing results mainly consider the motion characteristics of the structural parts and the energy distribution characteristics of the hydraulic support system under different loading modes. However, these studies did not consider the synergistic load-bearing effect of the coupled mechanical-hydraulic system of the hydraulic support. There is no comprehensive consideration of the influence of parameter changes on the bearing capacity of the support. Therefore, this paper comprehensively considers the working law of the double telescopic column of the hydraulic support,

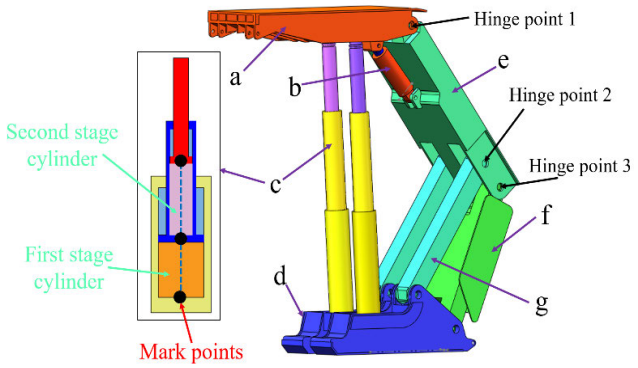

FIGURE 2. Mark points setting location. a: Top beam; b: Balance jack; c: Column; d: Bedplate; e: Shield beam; f: Rear link; g: Front link.

solves the problem that the mechanical and hydraulic cannot be coupled through the multi-software joint method, and establishes the co-simulation model of the hydraulic support. In addition, the differential response of the hydraulic support under different parameters is discussed by varying the roof rotary velocities and the relief valve flow rate.

II. ESTABLISHMENT OF HYDRAULIC SUPPORT MECHANICAL-HYDRAULIC CO-SIMULATION MODEL

A. ESTABLISHMENT OF MECHANICAL SYSTEM SUBMODEL

The two-column support usually shows stronger adaptability to the surrounding rock. Its single-row column support method can avoid the stability problem of the support caused by the front and rear columns. The key variables of support are indicated in Table 1.

Firstly, according to the working principle of the hydraulic support and the positional relationship of the structural parts, this section establishes the mechanical sub-model of the hydraulic support using ADAMS. The constraint relationship of each structural component is determined. The base is a fixed pair constraint, the hydraulic cylinder is a dynamic pair constraint, and the connecting parts of other parts are wheel set constraints. Secondly, the mark points are built to achieve real-time variable data interaction between different software. This step is used to complete the creation of state signals such as force, speed, and displacement of hydraulic cylinders. The mark points setting positions are indicated in Fig. 2.

B. ESTABLISHMENT OF HYDRAULIC SYSTEM SUBMODEL

Fig. 3A shows the hydraulic system diagram, where (a) is the hydraulic system sub-model built by AMESim, and (b) is the hydraulic system schematic diagram. The names and distribution locations of the components of the hydraulic system are clearly indicated by the mutual correspondence of the schematic diagram and the model diagram. The hydraulic component size setting reference is shown in Table 1. In (a), the data coupling module is used to exchange data with the mechanical system module, and the dimension gain module

TABLE 1. Key variables of support.

Key variables	Numerical magnitude
Height /m	3.8 to 8.2
Width /m	1.9 to 2.2
Setting load /kN	16544
Working pressure /MPa	37.5
Working force /kN	21000
First stage cylinder /m	External diameter (0.56)，Internal diameter (0.53)，Length (2.11)
Second stage cylinder /m	External diameter (0.38)，Internal diameter (0.35)，Length (2.19)
Balance jack hydraulic cylinder /m	External diameter (0.32)，Internal diameter (0.23)，Length (0.56)
Relief valve type	FAD 1000/50
Hydraulic operated check valve type	FDY 1000/50

is used to match the units between different variables. Fig. 3B shows the flowchart of simulation modeling. After the above process, the established mechanical system and hydraulic system variables are imported into Simulink, which can generate and connect the two system modules, completing the data exchange between different software. Before the simulation, the key parameters are set as follows. The compilation environment is set to C++, and the analysis type is nonlinear. Animation mode is interactive, simulation mode is discrete, and the communication interval is 0.0001 s. The Simulink solver selects the variable step size ode45. Simulation results of different systems can be obtained after completing the simulation.

C. HYDRAULIC SUPPORT LIFTING PROCESS RESULTS ANALYSIS

This section analyzes the lifting movement of the hydraulic support by considering the influence of its gravity and ignoring the external load. The positions of the first stage cylinder and second stage cylinder in the column system are shown in Fig. 2. To facilitate the reader's understanding, the height change process of the hydraulic support is divided into three stages: 0 s to 2 s for stage 1, which is the process of the first stage cylinder piston rising; 2 s to 8.61 s for stage 2, which is the process of the second stage cylinder piston rising; 8.61 s to 12 s for stage 3, which is the stage when the pressure of the lower chamber of the column reaches the pumping station pressure (37.5 MPa).

According to Fig. 4A, the column inlet switch is always open. Furthermore, the balance jack inlet switch is always closed, which is in the adaptive balance state. According to Fig. 4 (B-E), In stage 1, the high-pressure oil enters the first stage cylinder (1500L/min). With the increase of oil pressure, the first stage cylinder piston is pushed up (the rising distance is 2.11 m). The height of the support increases from 6.9 m to 7.15 m. In stage 2, when the first stage cylinder piston moves to the end of the stroke, the oil enters the second stage cylinder (1500L/min) smoothly and continues to push

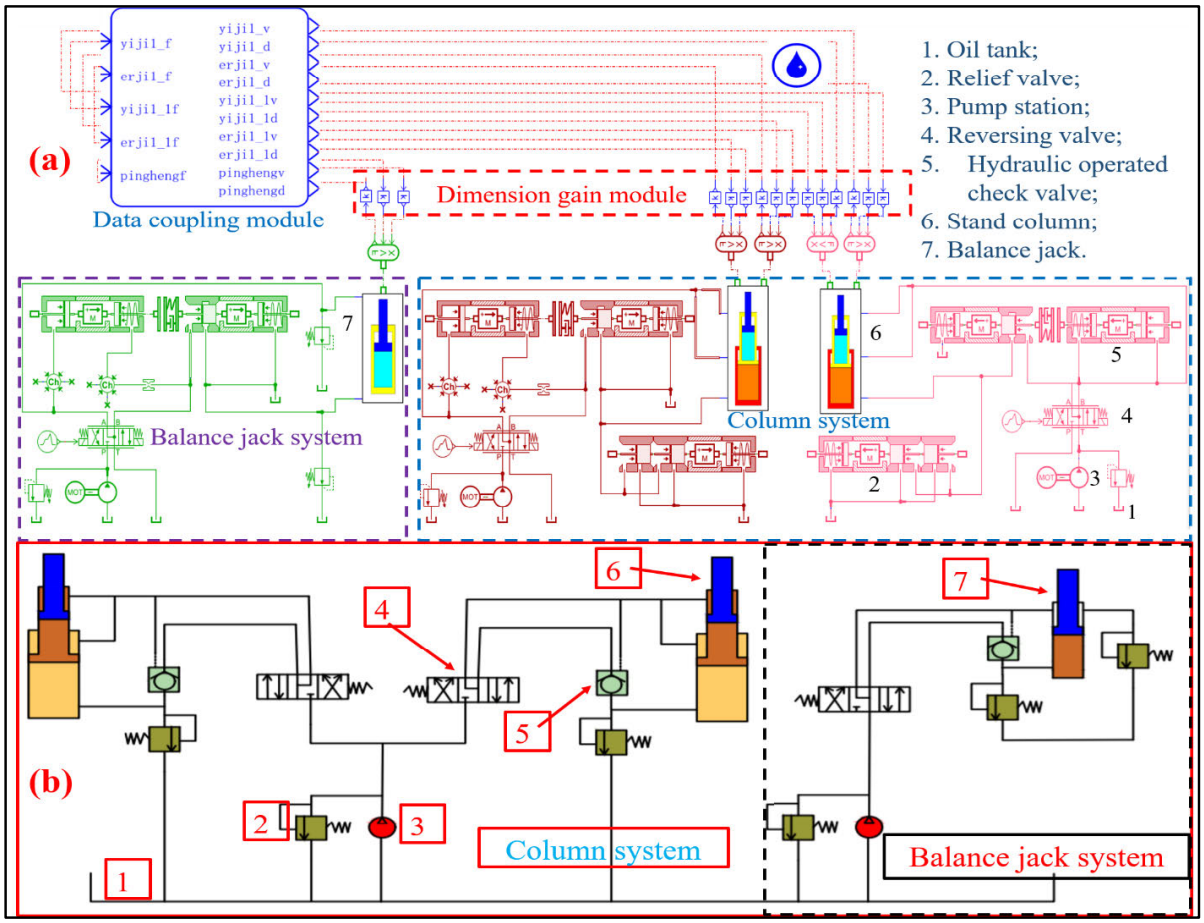

(a)

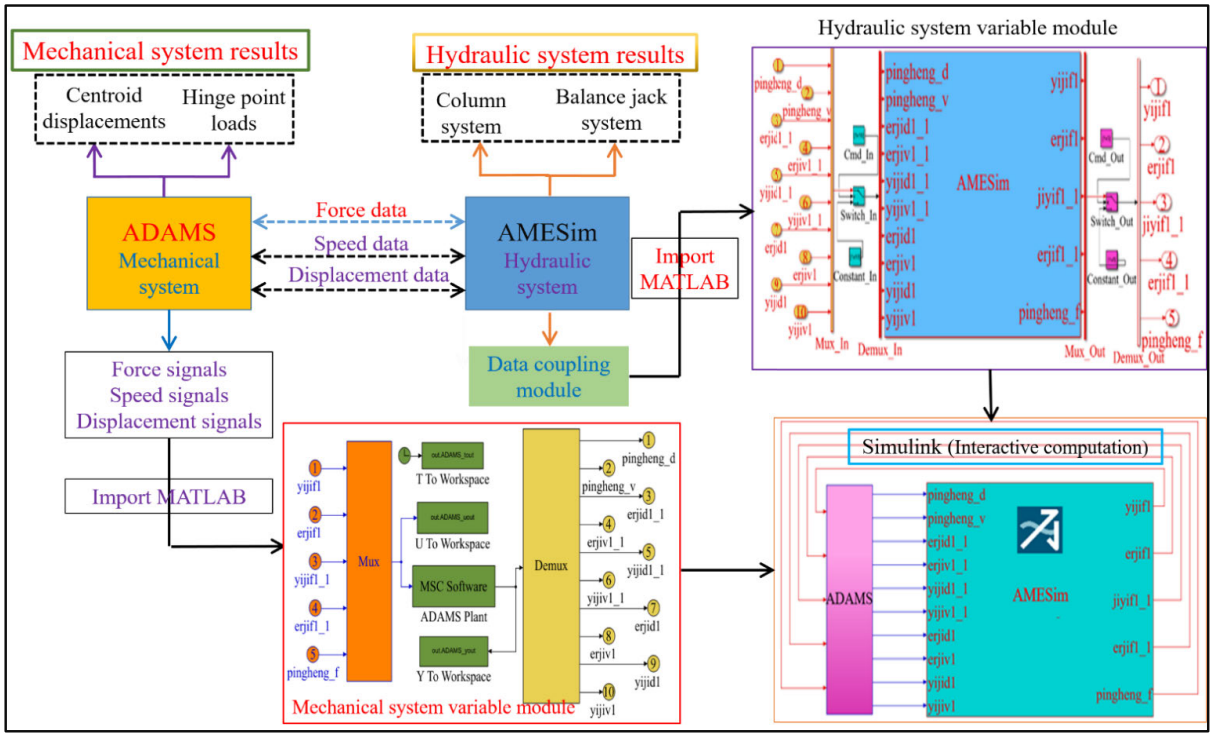

(b)

FIGURE 3. (a) Hydraulic system diagram. (a): Hydraulic system sub-model. (b): Hydraulic system schematic diagram. (b) The flowchart of simulation modeling.

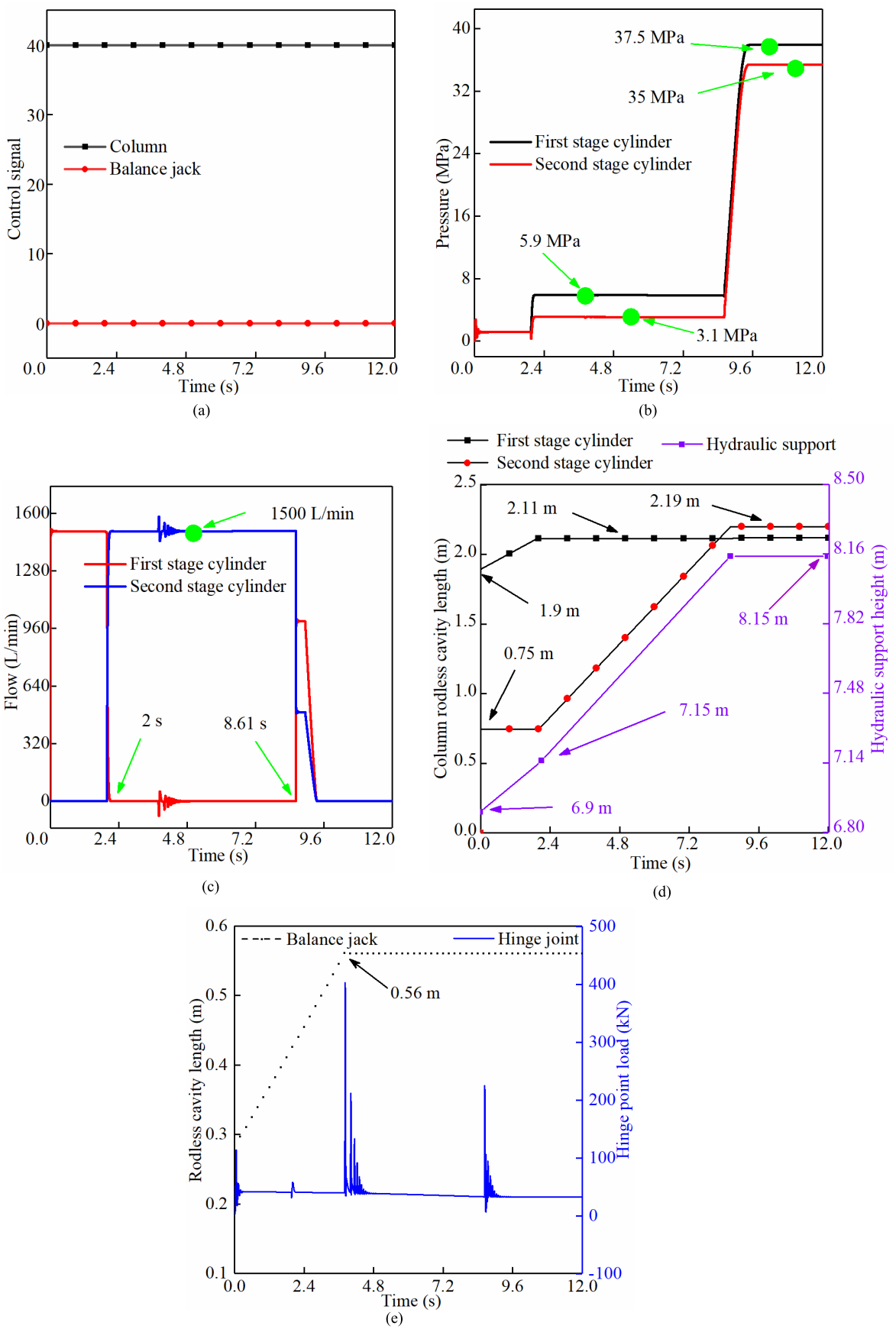

FIGURE 4. (a) Column and balance jack control signal. (b). Column hydraulic cylinder pressure. (c) Column hydraulic cylinder flow. (d). Column rodless cavity length and hydraulic support height. (e) Balance jack rodless cavity length and hinge point load.

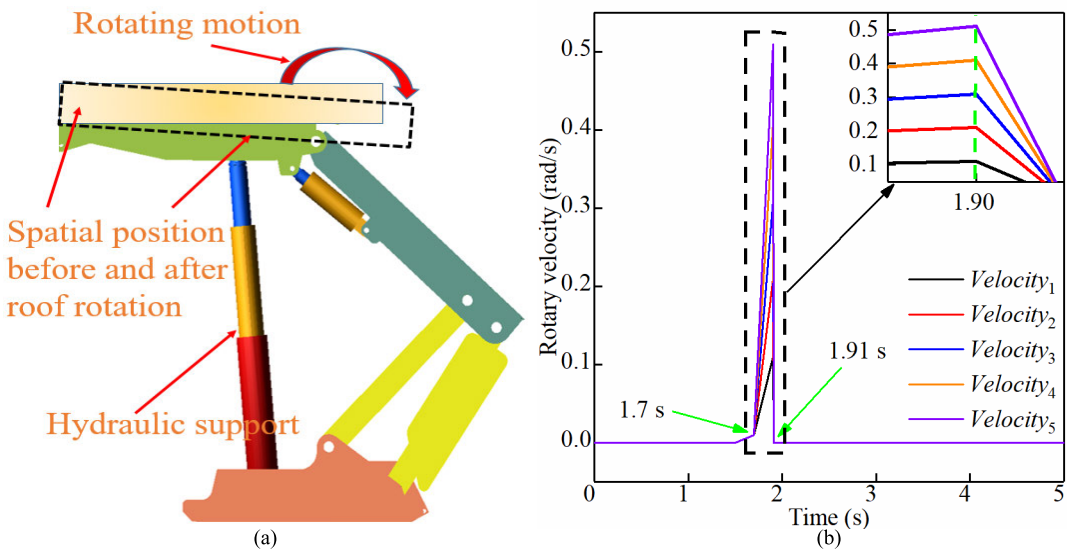

FIGURE 5. (a) Roof rotary load adding method. (b). Different roof rotary velocities.

the second stage cylinder piston up (the rising distance is 2.19 m). The height of the support increases from 7.15 m to 8.15 m in this process. In stage 3, after the height of the support reached the maximum, the pressure inside the column chamber gradually increased and finally reached the pumping station pressure (37.5 MPa). The height of the support no longer varies. The length of the rodless cavity of the balance jack is also gradually stretched with an increase in the support height (the longest is 0.56 m at 3.84 s). Due to the stop of the balance jack piston movement, the overall motion state of the hydraulic support also changed. At 3.84 s, the flow curve of the column lower chamber fluctuates. In addition, with the change in the lengths of the column, the hinge point load also shows a significant change. The hinge point load is the largest (40 kN) at 3.84 s.

Based on the above analysis, this section takes the column system as the active member and other structural members as the follower. The influence law of column piston motion on the change of support height is obtained. This shows that the method of mechanical-hydraulic co-simulation adopted is reasonable. Moreover, the results of the mechanical system and hydraulic system can be obtained after the simulation. This can provide the analysis model for the subsequent acquisition of the dynamic response of the support under different working conditions.

III. RESPONSE ANALYSIS OF HYDRAULIC SUPPORT UNDER ROOF ROTATION

A. THE METHOD OF ROOF ROTARY LOADING ADDITION

Under working conditions, the hydraulic support is in the' basic roof - upper immediate roof - hydraulic support -floor' coupling system [28], [29]. Influenced by the rock stiffness and support strength, the rotary speed of the roof after fracture is different, and the impact effect on the support is also different. The direct roof and the basic roof are uniformly defined as the rigid roof to simplify the model establishment. The position of the roof in space is above the top beam and behind the coal wall, where the collision force is set between the top beam and the roof, and the rotating pair is set between the roof and the coal wall. The roof rotation loading method is shown in Fig. 5A.

Affected by factors such as fracture location and rotary space; roof fracture will produce impact loads at different speeds. Therefore, it is meaningful to consider the influence of roof movement on hydraulic support. Since there is no regularity in the time and magnitude of the load acting on the support, it is difficult to accurately capture the transient response of the hydraulic support under the impact load. Therefore, this paper controls the rotary motion of the roof by applying the slewing function and then obtains the dynamic law of the support. To ensure the safety of the coal mining process, the hydraulic support should give the coal seam active support force in 0 s $\sim$ 1.7 s. This process keeps the spatial position of the roof fixed. The oil from the pumping station enters the column's lower chamber and when the support reaches the initial force, hydraulic oil is no longer required to enter the rodless column chamber. From 1.7 s to 1.9 s, five roof rotary velocities are set, and these velocities are named sequentially $Velocity_1$, $Velocity_2$, $Velocity_3$, $Velocity_4$, and $Velocity_5$. The peak velocity increases from 0.1 rad/s to 0.5 rad/s (interval is 0.1 rad/s,). From 1.90 s to 1.91 s, the rotary velocity is reduced to 0, and the position of the roof remains unchanged after rotation [14]. Furthermore, the simulation operation time of the process is set to 5 s. Different roof rotary velocity curves are shown in Fig. 5B.

B. EFFECT ON THE PRESSURE AND FLOW OF THE COLUMN SYSTEM

According to Fig. 6, the hydraulic support provides active support force in 0 s $\sim$ 1.7 s. During this period, the oil enters

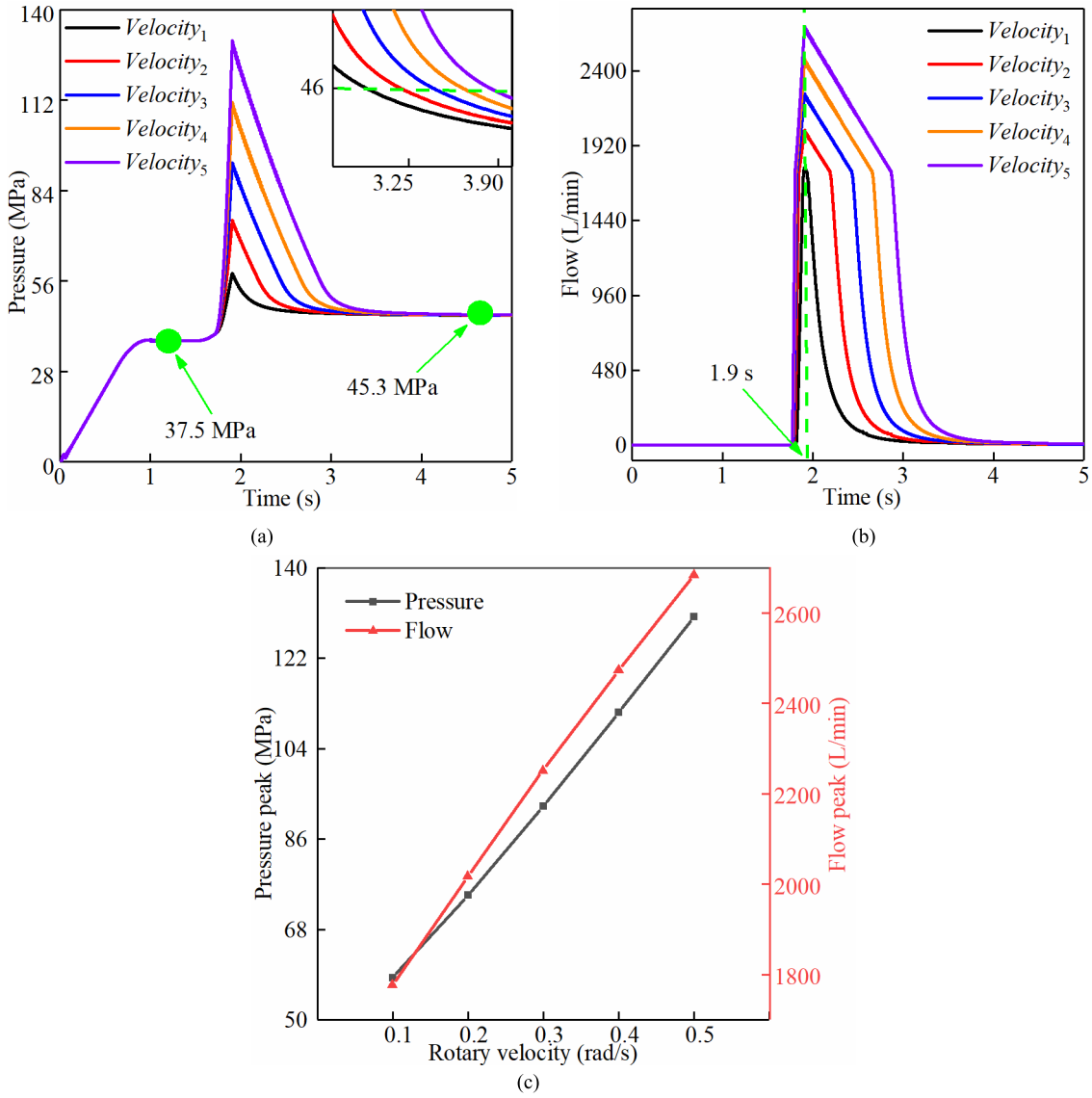

FIGURE 6. (a) Column pressure under different roof rotary velocities. (b) Column flow under different roof rotary velocities. (c). Column pressure and flow peak under different roof rotary velocities.

the rodless cavity of the column and pushes the piston of the column to rise. Due to the small impact on the support system when the oil enters, the curve has no large fluctuation and finally stabilizes at 37.5 MPa. The column pressure does not reach the opening pressure of the relief valve (the opening pressure is 45 MPa). Therefore, the flow curve does not change.

According to Fig. 6C, the pressure and flow peaks show an increasing trend as the rotary velocity increases. The peak pressure increases from 58.4 MPa to 130.3 MPa (with an increase of 123%), and the peak flow rate increases from 1776.5 L/min to 2683.8 L/min (with an increase of 51%). After the roof rotary velocity disappears, the chamber pressure and flow carve show a regular decrease and stability. When the impact load comes, the insufficient flow of the relief valve makes the high-pressure oil inside the column system unable to be released in time. Taking the *Pressure*(46 MPa) of the column as the reference pressure, the required time to reach *Pressure* (46 MPa) when $Velocity_1$ (0.1 rad/s) is 2.94 s, while the required time for $Velocity_5$ (0.5 rad/s) is extended to 3.83 s.

With the increase of the rotary speed of the roof, the impact load acting on the support increases, which makes the pressure and flow rate of the column rise gradually. Due to the small relief capacity of the relief valve, there is an extended unloading time.

C. EFFECT ON CENTROID DISPLACEMENT OF EACH STRUCTURAL COMPONENT

The spatial position of each structural component of the mechanical system is affected by the lengths of the column. Furthermore, the extension length of the column is

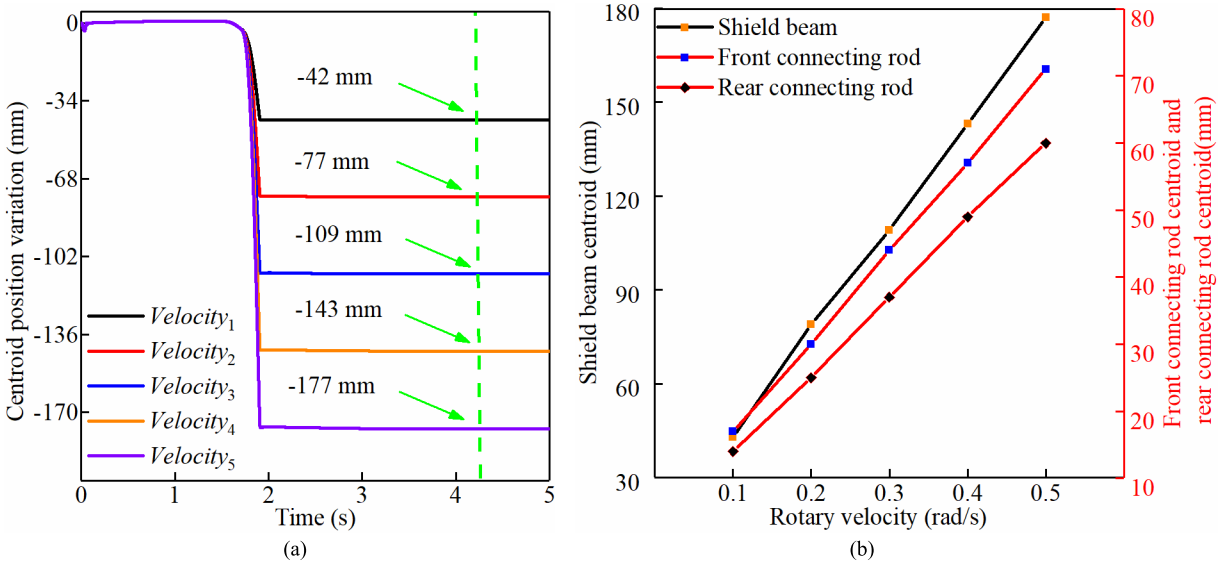

FIGURE 7. (a) Top beam centroid displacement under different roof rotary velocities. (b). The remainder of centroid displacement variation under different roof rotary velocities.

determined by the oil volume of the rodless cavity. Therefore, the migration states of each structural component will also alter with the change of the column system overflow volume under the action of roof rotation. The centroid displacement changes of each structural component in the vertical direction can be obtained from Fig. 7. The centroid displacement of the top beam in Fig. 7A is negative, which indicates the downward distance of the top beam centroid relative to the initial position. The value of the center of mass displacement in Fig. 7B is positive, which indicates the change of the other structure centroids relative to the initial position (the absolute value of the downward displacement). From 0 s to 1.7 s, the oil from the pump station enters the column lower chamber, and the piston starts to rise and drive the spatial position of the structural components to change. Since the roof and the top beam are in close contact, the roof height remains unchanged, and the upward movement of the top beam is blocked. Therefore, the centroid positions of each structural component do not change significantly during this period.

From 1.7 s to 1.9 s, an increase in rotary velocity makes the variation of each component centroid different after stabilization. The greater the rotation velocity, the greater the overflow volume of the column and the change in each component centroid. By comparing the variation of each structural component centroid, it can be found that the variation of these centroids increases five times when the rotary velocity increases to $Velocity_5$(0.5 rad/s). The above results show that when the load impacts the hydraulic support, the pressure in the lower chamber of the column begins to rise and gradually rises to 45MPa. At this time, the high-pressure oil begins to flow out through the relief valve, the elongation of the column piston decreases, and the spatial position of the structural parts also changes.

Based on the above analysis, the movement of the structural members is related to the elongation of the column piston. With the increase of the rotary speed of the roof, the pressure of the column reaches the opening pressure of the relief valve. The increase in the flow of the relief valve makes the piston retraction distance of the column rise, which leads to the overall height of the support decreasing. The displacement of the structural members' centroid of the mechanical system increasing.

D. EFFECT ON HINGE POINT LOAD

As a multi-link mechanism, the hinge points make the movement of structural parts affect each other. Moreover, the movement of the structure also changes the load of the hinge point [30], [31]. The top beam and the shield beam hinge point, the shield beam and the front link hinge point, and the shield beam and the rear link hinge point are defined as hinge point 1, 2, and 3, respectively. The positions of the hinge point are shown in Fig. 2. The load curves of the hinge point are shown in Fig. 8.

According to Fig. 8A, the force curves of the three hinge points show a trend of gradually increasing to a stable state from 0 s to 1.7 s. Loads of hinge points 1, 2, and 3 are stable at 8500 kN, 11700 kN, and 4100 kN, respectively. From 1.7 s - 5 s, the load at each hinge point rapidly increases to the peak and then gradually decreases to a stable value as the impact force decreases (the stability time is about 4.1 s). Under the given roof rotary velocity, the hinge point 2 has the highest peak load and hinge point 1 has the lowest peak load. According to Fig. 8B, the curve of changing trend of the hinge point 1 is the same under different roof rotation velocities. In a short period of rotation velocity change, the peak load at hinge points 1 increased 2.15 times (increased from 15,700 kN to 33,700 kN). The energy dissipation time of

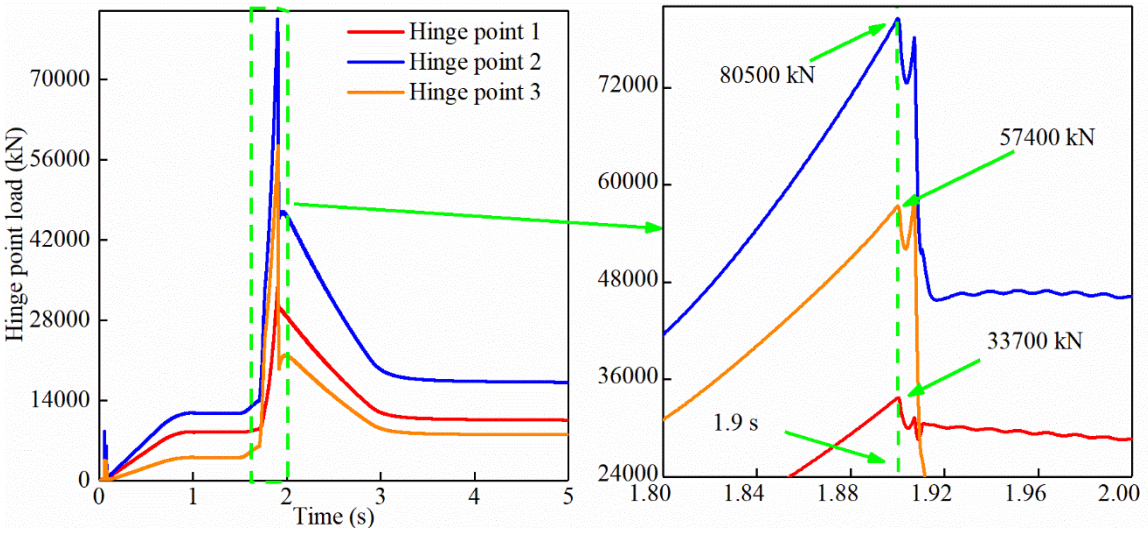

(a)

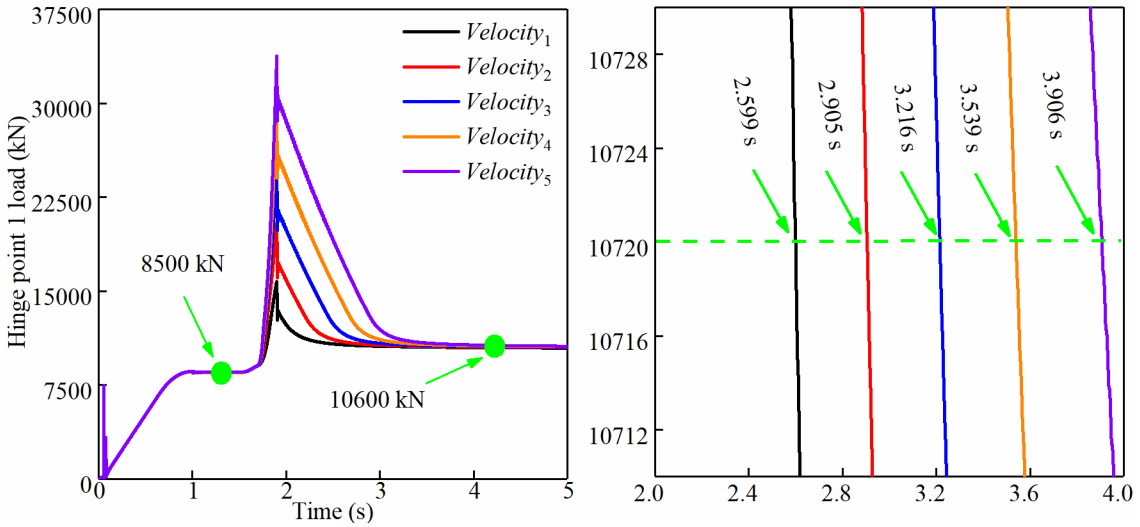

(b)

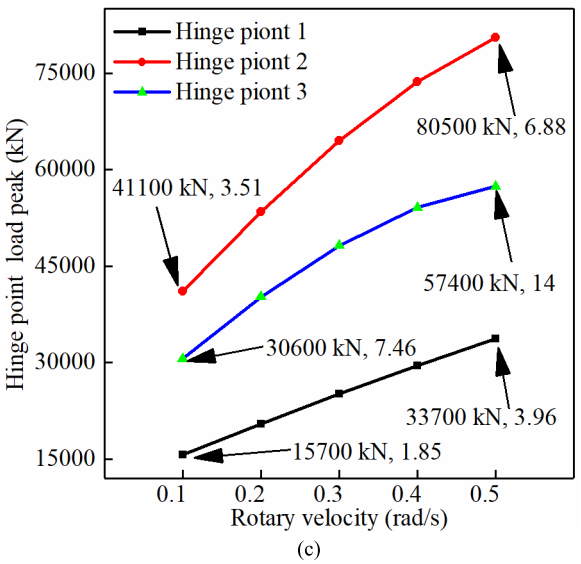

(c)

FIGURE 8. (a) Hinge point load of different positions at Velocity$_5$ (0.5 rad/s). (b). Hinge points 1 load under different roof rotary velocities. (c). Hinge point load growth rate of different positions under roof rotary velocities.

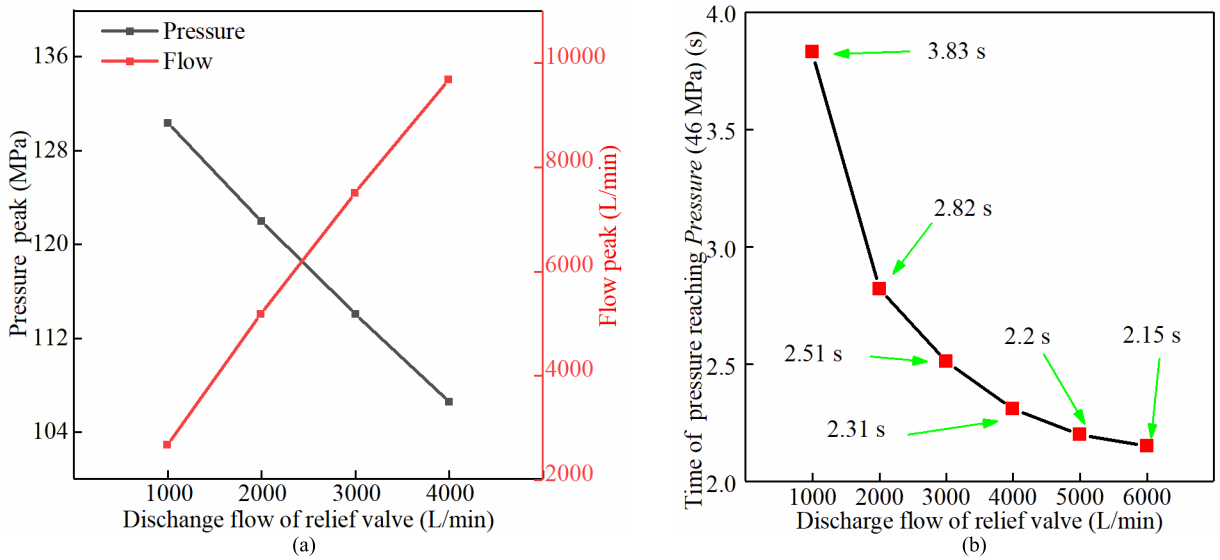

FIGURE 9. (a) Column pressure and flow peak under different discharge flows. (b). Times of pressure reaching Pressure (46 MPa) under different discharge flows.

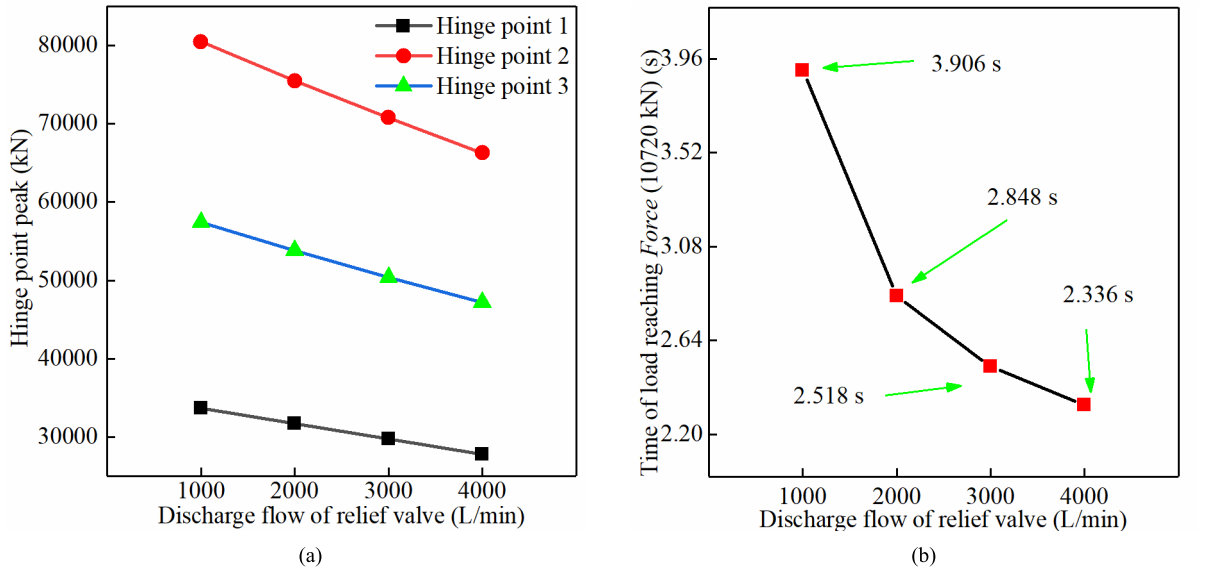

FIGURE 10. (a) Hinge point peak under different discharge flows. (b). Times of load reaching Force (10720 kN) under different discharge flows.

the column is prolonged under the existing relief valve flow after the velocity disappears. This also leads to the relative extension of the load stationary time of the hinge point 1. Taking *Force*(10720 kN) as the reference load, the time when a load of hinge point 1 reaches *Force* (10720 kN) is delayed by about 1.5 s. The change law of the load curve of hinge points 2 and 3 is the same as that of hinge point 1.

The ratio between the peak load and the stable load in the initial support stage under the impact of the roof rotation is defined as the load growth rate of the hinge point. This parameter is used to observe the sensitivity of the hinge point at different roof rotation velocities. According to Fig. 8C, when the rotary velocity is $Velocity_1$(0.1 rad/s), the load growth rates of hinge points 1, 2, and 3 are 1.85, 3.51, and 7.46, respectively. When the rotation velocity increases to $Velocity_5$(0.5 rad/s), the load growth rates increase by 3.96, 6.88, and 14, respectively. Therefore, with an increase in the rotary velocity, the load growth ratio of hinge point 3 is the most obvious, and the load growth ratio of hinge point 1 is the smallest. Therefore, hinge point 3 is the most sensitive to the change in roof rotary velocity.

As the connection point in the mechanical system, the load change condition of the hinge point is influenced by the movement law of the structural parts. Based on the above

analysis, the increase in the rotary speed of the roof changes the spatial position of the structural members, making the hinge point in the mechanical system a load-sensitive area, which may shorten the normal service life of the hydraulic support.

IV. EFFECT OF RELIEF VALVE NUMBER ON HYDRAULIC SUPPORT ENERGY UNLOADING

When the pressure under the column cavity is too large, the relief valve will overflow the flow to ensure the stability of the column system. At the same time, the frequent occurrence of mine anomalies also puts forward higher requirements for the relief valve [32], [33]. The above simulation results show that the relief valve connected with the lower chamber of the column has the problem of small overflow flow, which prolongs the release time of high-pressure oil and hinders the energy release of the system. Therefore, this section discusses column system changes by adjusting the flow of the relief valve (the roof rotary velocity is selected as $Velocity_5$(0.5 rad/s)).

A. EFFECT ON COLUMN SYSTEM ENERGY UNLOADING

When the roof rotation speed is the same, the column system has the same overflow flow through the relief valve. However, adding the discharge flow of relief valves can change the overflow speed of the column to shorten the overflow time.

According to Fig. 9A, the flow of relief valves changes from 1000 L/min to 4000 L/min. The pressure peak differences between the adjacent curves are 8.33 MPa, 7.91 MPa, and 7.51 MPa. The flow peak differences are 2503.7 L/min, 2322.8 L/min, and 2167.4 L/min, and the differences in the required time to reach *Pressure* (46 MPa) are 1.01 s, 0.31 s, and 0.2 s. The column system can greatly reduce the pressure and increase the overflow by adding the discharge flow. However, the change in the energy dissipation of the column system is weakened. The flow of relief valves is added to 6000 L/min to further analyze the effect of the relief valve flow on the energy consumption of the column. According to Fig. 9B, the time when the rodless chamber pressure reaches the *Pressure* (46 MPa) is reduced, but the reduction is lower. Therefore, adding the discharge flow of the relief valve can reduce the pressure, increase the flow rate, and shorten the required time for the pressure to reach *Pressure*(46 MPa). However, when the impact load is constant, the overflow effect of the rodless cavity gradually weakens with the addition of the discharge flow of the relief valve.

Based on the above analysis, when the relief valve flow is insufficient, it cannot quickly overflow the oil from the column, which will hinder the release of energy. Increasing the relief valve relief flow not only speeds up the overflow of the column cavity but also increases the overflow. It changes the situation that the pressure in the column chamber is too high.

B. EFFECT ON LOAD PEAK OF HINGE POINT

The deflection angle of the roof at the same rotary velocity is constant; thus, the positions that each structural component of the hydraulic support can migrate in space are determined. Adding the discharge flow of the relief valve can change the overflow speed of the column. Therefore, the speed of each structural component to the specified position becomes faster. The variation trend of hinge point load also changes. According to Fig. 10A, with an increase in the discharge flow of relief valves, load reduction amplitudes of hinge points 1, 2, and 3 are 17.5%, 17.6%, and 17.8%, respectively. According to Fig. 10B, adding the discharge flow of relief valves makes the time of hinge points 1 reaching *Force*(10720 kN) shorter by about 1.77 s. When the roof rotary velocity is constant, the discharge flow of the relief valve increases greatly, while the change in the time required to reach *Force* (10720 kN) decreases gradually. Therefore, the discharge flow of relief valves should be selected according to the actual working conditions.

The load at the articulation point reflects the force of the hydraulic support. The increase of the relief valve relief flow changes the load distribution of the mechanical system, making the load at the critical position less sensitive to the sudden change of load. The working reliability of the support is enhanced.

V. CONCLUSION

This paper took the two-column hydraulic support and established the co-simulation model. The dynamic response characteristics were analyzed by changing the roof rotary velocity and the discharge flow of relief valves.

1. Based on the establishment of the co-simulation model, the movement process of the hydraulic support was discussed. Furthermore, the system pressure, flow variation characteristics, and hinge point load were analyzed. Compared with the analysis of a single hydraulic system and mechanical system, the mechanical-hydraulic co-simulation model can more comprehensively observe the cooperative work of hydraulic support.

2. With an increase in the roof rotary velocity (from 0.1 rad/ s to 0.5 rad/ s), the pressure peak of the rodless cavity at the adjacent two rotary velocities increases almost steadily, and the flow peak increases by 51%. The limited discharge flow of the relief valve slowed down the overflow speed of the column rodless cavity. Lastly, the energy release time of the column system was also extended by more than 1 s.

3. With an increase in the rotary velocity, the centroid position of each structural component changed in the vertical direction and increased by five times. Furthermore, the hinge point loads at different positions also changed differently. Among them, the load peak of hinge point 2 was the highest. The load peak of hinge point 3 was more sensitive (the load growth rate is 14). Therefore, the dangerous zone of structural parts appeared in the connection position of the front and rear connecting rod and shield beam under the action of rotating roof load.

4. The pressure peak in the column decreased by 18.5%, the flow peak increased by 260%, and the required time to reach the reference pressure was about 1.5 s shorter by

adding the discharge flow of the relief valve. The load of hinged points at different positions decreased significantly by 17% on average. However, the discharge effect of the hydraulic system changed little. Therefore, the type of relief valve should be selected reasonably according to the size of the mine pressure.

Due to lack of time, the flexible treatment of the hydraulic support was not accounted for in this paper. Moreover, minor deformation of hydraulic support structural components due to load impact that alters force transfer characteristics was also not considered. Therefore, the above deficiencies can be discussed in the follow-up work.

REFERENCES

[1] J. Hou, C. Li, L. Yuan, J. Li, and F. Liu, "Study on green filling mining technology and its application in deep coal mines: A case study in the Xieqiao coal mine," *Frontiers Earth Sci.*, vol. 10, p. 2488, Jan. 2023, doi: 10.3389/FEART.2022.1110093.

[2] D.-J. Ma, L.-R. Wan, K.-D. Gao, Q.-L. Zeng, and X.-M. Wang, "The meshing and failure analysis of haulage wheels with the effect by shearer's poses," *Eng. Failure Anal.*, vol. 137, Jul. 2022, Art. no. 106251, doi: 10.1016/J.ENGFAILANAL.2022.106251.

[3] Y. Yang, Q. Zeng, L. Wan, and G. Yin, "Influence of coal gangue volume mixing ratio on the system contact response when multiple coal gangue particles impacting the metal plate and the study of coal gangue mixing ratio recognition based on the metal plate contact response and the multi-information fusion," *IEEE Access*, vol. 8, pp. 102373–102398, 2020, doi: 10.1109/ACCESS.2020.2997987.

[4] H. Chu, G. Li, Z. Liu, X. Liu, Y. Wu, and S. Yang, "Multi-level support technology and application of deep roadway surrounding rock in the Suncun Coal Mine, China," *Materials*, vol. 15, no. 23, p. 8665, Dec. 2022, doi: 10.3390/MA15238665.

[5] D. Ma, L. Wan, X. Zhang, Q. Zeng, and K. Gao, "Meshing characteristics and failure analysis of shearer walking wheel considering torsional deformation," *Alexandria Eng. J.*, vol. 61, no. 7, pp. 5771–5782, Jul. 2022, doi: 10.1016/J.AEJ.2021.09.035.

[6] Z. Qiang, K. Yang, J. Zhang, Y. Wei, X. Liu, Z. Wu, W. Song, and X. Xiling, "Monitoring and measurement analysis of key indexes for the implementation of mining, dressing, backfilling, and controlling technology in coal resources—A case study of Tangshan mine," *Energy Sci. Eng.*, vol. 10, no. 3, pp. 680–693, Mar. 2022, doi: 10.1002/ese3.1057.

[7] K. Gao, W. Xu, H. Zhang, Y. Zhang, Q. Zeng, and L. Sun, "Relative position and posture detection of hydraulic support based on particle swarm optimization," *IEEE Access*, vol. 8, pp. 200789–200811, 2020, doi: 10.1109/ACCESS.2020.3035576.

[8] Q. Zeng, Y. Yang, X. Zhang, L. Wan, J. Zhou, and G. Yin, "Study on metal plate vibration response under coal–gangue impact based on 3D simulation," *Arabian J. Sci. Eng.*, vol. 44, no. 9, pp. 7567–7580, Sep. 2019, doi: 10.1007/s13369-019-03853-3.

[9] D. Szurgacz, "Analysis of the pressure increase in the hydraulic cylinder of the longwall powered roof support during use," *Appl. Sci.*, vol. 12, no. 17, p. 8806, Sep. 2022, doi: 10.3390/app12178806.

[10] D. Szurgacz and J. Brodny, "Analysis of the influence of dynamic load on the work parameters of a powered roof support's hydraulic leg," *Sustainability*, vol. 11, no. 9, p. 2570, May 2019, doi: 10.3390/su11092570.

[11] C. Guo, J. Mao, and M. Xie, "Analysis of energy absorption characteristics of corrugated top beams of anti-impact hydraulic supports," *Alexandria Eng. J.*, vol. 61, no. 5, pp. 3757–3772, May 2022, doi: 10.1016/j.aej.2021.08.077.

[12] Z. S. Meng, J. M. Zhang, Y. Y. Xie, Z. G. Lu, and Q. L. Zeng, "Analysis of the force response of a double-canopy hydraulic support under impact loads," *Int. J. Simul. Model.*, vol. 20, no. 4, pp. 766–777, Dec. 2021, doi: 10.2507/IJSIMM20-4-CO18.

[13] C. Guo, "Analysis of pressure regulating characteristics of safety valve in hydraulic system of offshore oil production equipment," *Ain Shams Eng. J.*, vol. 13, no. 5, Sep. 2022, Art. no. 101738, doi: 10.1016/J.ASEJ.2022.101738.

[14] G. Zhao, H. Wang, Y. Song, and C. Zhang, "Dynamic characteristics study on the two-stage safety valve used on hydraulic support under impact loading," *J. Theor. Appl. Mech.*, vol. 58, no. 3, pp. 623–635, Jul. 2020, doi: 10.15632/jtam-pl/116576.

[15] Z. Meng, Q. Zeng, K. Gao, S. Kong, P. Liu, and L. Wan, "Failure analysis of super-large mining height powered support," *Eng. Failure Anal.*, vol. 92, pp. 378–391, Oct. 2018, doi: 10.1016/j.engfailanal.2018.04.011.

[16] G. Li, L. Li, B. Guo, and Y. Li, "Design of a high water-based fluid, high-pressure, and large-flow safety valve," *J. Eng.*, vol. 2019, no. 13, pp. 79–85, Jan. 2019, doi: 10.1049/joe.2018.8972.

[17] A. Pytlik, "Process characteristics of hydraulic legs equipped with safety valves at dynamic load caused by a mining tremor," *Arch. Mining Sci.*, vol. 60, no. 2, pp. 595–612, Jun. 2015, doi: 10.1515/amsc-2015-0039.

[18] Z. K. Yang, Z. Y. Sun, S. B. Jiang, Q. H. Mao, P. Liu, and C. Z. Xu, "Structural analysis on impact-mechanical properties of ultra-high hydraulic support," *Int. J. Simul. Model.*, vol. 19, no. 1, pp. 17–28, Mar. 2020, doi: 10.2507/IJSIMM19-1-498.

[19] L. Wan, J. Wang, D. Ma, Q. Zeng, Z. Li, and Y. Zhu, "Vibration response analysis of hydraulic support based on real shape coal gangue particles," *Energies*, vol. 15, no. 5, p. 1633, Feb. 2022, doi: 10.3390/en15051633.

[20] H. Ren, D. Zhang, S. Gong, K. Zhou, C. Xi, M. He, and T. Li, "Dynamic impact experiment and response characteristics analysis for 1:2 reduced-scale model of hydraulic support," *Int. J. Mining Sci. Technol.*, vol. 31, no. 3, pp. 347–356, May 2021, doi: 10.1016/j.ijmst.2021.03.004.

[21] Z. Fugang, Y. Long, S. Di, L. Ruiyang, and T. Wei, "Simulation analysis of dynamic characteristics and influencing factors of hydraulic work support based on AMESim," in *Proc. IEEE 8th Int. Conf. Fluid Power Mechatronics (FPM)*, Apr. 2019, pp. 981–986.

[22] A. Sheela, M. Atshaya, S. Revathi, and N. J. Singh, "Investigation on PMSM for electric vehicle applications using co-simulation of MATLAB and magnet software," *IOP Conf. Ser., Mater. Sci. Eng.*, vol. 1055, no. 1, Feb. 2021, Art. no. 012138, doi: 10.1088/1757-899X/1055/1/012138.

[23] I. M. Khan, M. Datar, W. Sun, G. Festag, T. B. Juang, and N. Remisoski, "Multibody dynamics cosimulation for vehicle NVH response predictions," *SAE Int. J. Vehicle Dyn., Stability, NVH*, vol. 1, no. 2, pp. 131–136, Mar. 2017, doi: 10.4271/2017-01-1054.

[24] T. Duyun, I. Duyun, L. Rybak, and V. Perevuznik, "Simulation of the structural and force parameters of a robotic platform using co-simulation," *Proc. Comput. Sci.*, vol. 213, pp. 720–727, Jan. 2022, doi: 10.1016/J.PROCS.2022.11.126.

[25] D. Pan, S. Gu, G. Guo, H. Kuang, H. Zhong, and F. Gao, "Co-simulation design and experimental study on the hydraulic–pneumatic-powered driving system of main steam and feed water isolation valves for CAP1400," *Adv. Mech. Eng.*, vol. 9, no. 8, Aug. 2017, Art. no. 168781401772007, doi: 10.1177/1687814017720078.

[26] A. Ebadi and M. A. Sh, "Dynamic simulation of a one DOF radial active magnetic bearing using SIMULINK and AMESim co-simulation," *Int. J. Mater., Mech. Manuf.*, vol. 4, no. 3, pp. 162–166, 2015, doi: 10.7763/IJMMM.2016.V4.247.

[27] A. S. Nair and D. Ezhilarasi, "Performance analysis of super twisting sliding mode controller by ADAMS–MATLAB co-simulation in lower extremity exoskeleton," *Int. J. Precis. Eng. Manuf.-Green Technol.*, vol. 7, no. 3, pp. 743–754, May 2020, doi: 10.1007/s40684-020-00202-w.

[28] B. Wang, L. Mu, M. He, and S. Gu, "Mechanism analysis of roof deformation in pre-driven longwall recovery rooms considering main roof failure form," *Sustainability*, vol. 14, no. 15, p. 9093, Jul. 2022, doi: 10.3390/su14159093.

[29] Y. Tai, S. Guo, and K. Fang, "Research on the transition section length of the mixed workface using gangue backfilling method and caving method," *Open Geosci.*, vol. 11, no. 1, pp. 649–663, Oct. 2019, doi: 10.1515/geo-2019-0052.

[30] Q.-L. Zeng, Z.-S. Meng, L.-R. Wan, and C.-L. Wang, "Analysis on force transmission characteristics of two-legged shield support under impact loading," *Shock Vibrat.*, vol. 2018, pp. 1–10, Jan. 2018, doi: 10.1155/2018/3854684.

[31] H. X. Liu, R. Jia, Y. L. Li, and G. W. Gai, "Parameters solving and optimization of long working stroke hydraulic support mechanism using regional approximation and dynamic graphical solution," *J. Editorial Office Trans. Chin. Soc. Agricult. Eng.*, vol. 33, no. 4, pp. 1–9, 2017.

[32] X. F. He, L. J. Luo, X. L. Liu, and X. H. Luo, "Simulation on an experimental system for the dynamic characteristics of safety valves with high pressure and large flow rate," *Appl. Mech. Mater.*, vols. 263–266, pp. 748–755, Dec. 2012, doi: 10.4028/WWW.SCIENTIFIC.NET/AMM.263-266.748.

[33] C. Zhang, S. H. Zhao, G. Guo, and W. K. Dong, "Modeling and simulation of emulsion pump station pressure control system based on electro-hydraulic proportional relief valve," *J. Appl. Mech. Mater.*, vols. 190–191, pp. 263–266, Jul. 2012, doi: 10.4028/www.scientific.net/AMM.190-191.860.

QINGLIANG ZENG received the B.S. and M.S. degrees in mechanical engineering from the Shandong University of Science and Technology, Tai'an, China, in 1985 and 1988, respectively, and the Ph.D. degree from the China University of Mining and Technology, Beijing, China, in 2000. He is currently a Professor with the Department of Mechanical and Electronic Engineering, Shandong University of Science and Technology, and the Headmaster of Shandong Normal University. His current research interests include computer integrated manufacturing systems and mechanical-electrical-hydraulic integration.

CHEN MA was born in Shandong, China, in 2000. He received the B.S. degree in mechanical engineering from Linyi University, Linyi, China, in 2017. He is currently a Researcher in mechanical engineering with the Shandong University of Science and Technology. His research interests include hydraulic support, impact response, and mechanical-hydraulic cooperative.

ZHAOSHENG MENG received the Ph.D. degree in mechanical engineering from the Shandong University of Science and Technology, Qingdao, China, in 2018. He is currently a Vice Professor with the College of Energy and Mining Engineering, Shandong University of Science and Technology. His research interests include the mining machinery and mechanical-electrical-hydraulic integration.

PENGHUI XU received the bachelor's degree from the Shandong University of Science and Technology, Qingdao, China, in 2021, where he is currently pursuing the master's degree with the Mechanical and Electronic Engineering Department. His research interest includes mining machinery.

XIAOWAN LEI received the B.S. degree in mechanical engineering from the Shandong University of Science and Technology, Qingdao, China, in 2022. He is currently a Researcher in mechanical engineering with the Shandong University of Science and Technology. His research interests include hydraulic support impact response and coal-gangue identification.